KRONOS FUSION ENERGY

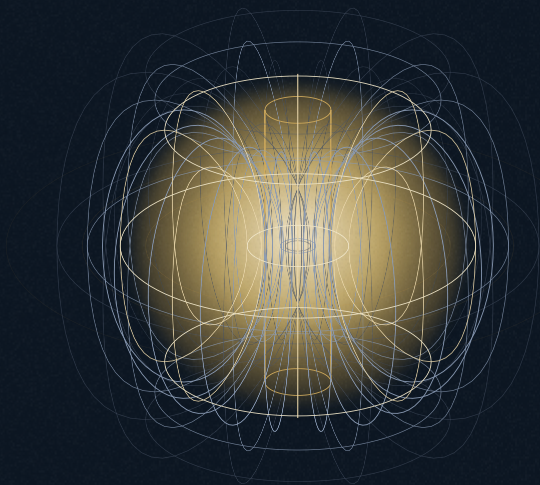

PAPER 2.3 · THE KRONOS 2026 SERIES

The Medical-Isotope Mission of a Compact Spherical-Tokamak Breeder: Mo-99, Targeted-Alpha Emitters, and Byproduct Isotope Co-Production on a 14 MeV Neutron Source

A tritium breeder is, before it is anything else, a bright and steady source of neutrons, and that source has value beyond breeding. We formalise the isotope-production and…

Read it live — 3-D model · physics validator · film series

BY P I FORD AND G L KULCINSKI

2026 · EDITORIAL EDITION

THE OFFICIAL RECORD

What this document is, and how to read its numbers

This is a combined editorial. It gathers, in one volume, the two design studies Kronos Fusion Energy released in 2026 — a compact spherical-tokamak tritium/helium-3 breeder and a deuterium–helium-3 tandem-mirror generator — together with the intellectual-property estate, the people, and, in the internal edition, the full commercial case. The scientific text is the same text that appears in the arXiv preprints and the journal submissions; the editorial adds the apparatus a reader needs to hold the whole program at once, and nothing in the physics is altered to fit it.

THE HONESTY STANCE IS THE ASSET

Every headline quantity carries an **evidence class** — DERIVED RECOMPUTED MEASURED REQUIREMENT — and, where a number is a modelled extrapolation rather than a demonstrated value, it is labelled as such and its downside is shown next to it. Several quantities in the underlying corpus moved after first publication; where a value has been withdrawn or restated, the record says so plainly. This is deliberate: a diligence team will find the load-bearing assumptions, so the document surfaces them first.

TWO EDITIONS

This volume is issued in two editions. The **public edition** (light) carries the physics and the design only — no dollar, price, or per-kilogram figure appears anywhere in it. The **internal edition** (dark) adds the economics, the funding architecture, and the defense-commercial analysis, and is marked *Confidential* accordingly; it is not for public distribution. Where the commercial case rests on a modelled assumption rather than a demonstrated one, it is labelled as such and its downside is shown alongside it, on the same terms as the physics.

TITLE	The Kronos Fleet — Hyperion · Aegis · MetroVolt: A Combined Design & Commercialization Study
AUTHOR	Priyanca Ford, Founder & CEO, on behalf of Kronos Fusion Energy
EDITION	2026 Combined Editorial · first issue
COMPANION WORKS	The five-paper arXiv drop — (1) Breeder, (2) Burner, (3) REBCO magnet & tape, (4) Direct Energy Conversion, (5) AI/ML/Quantum control — with matching numbered Zenodo deposits, plus the IOP journal and IAEA-FEC submissions. Patents were filed before the drop.
NAMING	Hyperion = the breeder; Aegis (defense) and MetroVolt (data-center) = one generator in two housings. Internal mode letters (D1, L) do not appear on public surfaces.
STATUS	Conceptual design & simulation study. Nothing herein is a construction commitment.

HOW TO READ THIS VOLUME

The fleet at a glance, and the way its numbers are marked

This volume opens with *Orientation*, presents the five research papers as a bound sequence, and closes with the *Apparatus*. *Foundations* sets out the three general results both machines rest on. *Paper One* is the Hyperion breeder; *Paper Two* the Aegis / MetroVolt generator; *Papers Three, Four and Five* are the enabling science — high-field REBCO magnets and tape, direct energy conversion, and the AI / ML / quantum control stack. A *Digital Twin & 3-D Model* part follows, then the *Environmental* profile. The *Economics* and levelized cost and the *Business Case* and diligence record appear in the internal edition only; the *Simulations* proof record and the Apparatus — patent portfolio, team, limitations, and sources — close both editions.

THE FLEET AT A GLANCE

	HYPERION	AEGIS	METROVOLT
Role	Strategic-isotope foundry	Defense installation power	Campus power
Machine	**Spherical tokamak**	**Tandem mirror**	**Tandem mirror**
Fuel	Deuterium–tritium	Deuterium–helium-3	Deuterium–helium-3
Delivers	Tritium · ^{3}He · 14 MeV n	Resilient installation power	Firm campus power
Physics bar	**Fusion gain only**	Closure (gates named)	Closure + lunar ^{3}He
In the fleet	Breeds the fuel	Proves the generator	Commercial destination

HOW THE NUMBERS ARE MARKED

Every headline quantity carries an evidence class — DERIVED from first principles, RECOMPUTED from raw data, MEASURED in hardware, or a REQUIREMENT yet to be met. Financial figures carry a case label and are confined to the internal (confidential) edition. Values that moved after first publication are shown as withdrawn or restated rather than quietly changed. A capability you can evaluate is one whose limits are on the page.

ABSTRACT

The Medical-Isotope Mission of a Compact Spherical-Tokamak Breeder: Mo-99, Targeted-Alpha Emitters, and Byproduct Isotope Co-Production on a 14 MeV Neutron Source

A tritium breeder is, before it is anything else, a bright and steady source of $14\,\mathrm{MeV}$ neutrons, and that source has value beyond breeding. We formalise the isotope-production and materials-qualification missions of the compact spherical-tokamak breeder (Hyperion) at its frozen operating point — fusion power $P_{\mathrm{fus}} = 85.04\,\mathrm{MW}$, gain $Q = 3.076$, plasma current $I_p = 9.66\,\mathrm{MA}$, negative triangularity $\delta = -0.30$ — which sustains a whole-device source strength $S_n = 3.009 \times 10^{19}\,\mathrm{n\,s^{-1}}$ and a first-wall fast flux of $7.0 \times 10^{14}\,\mathrm{n\,cm^{-2}\,s^{-1}}$. We derive the governing production and depletion equations, the two-step Bateman chain of the molybdenum-99/technetium-99m generator, the spectrum-folded reaction-rate integral, and a formal materials-qualification figure of merit, and we cast the source-strength/centrepost-damage coupling as a strict proportional constraint. On this basis a first-wall $^{100}\mathrm{Mo}(n, 2n)^{99}\mathrm{Mo}$ target with no moderator and no added hardware reaches a frozen end-of-bombardment activity of $\approx 1{,}981\,\mathrm{Ci}$ per $100\,\mathrm{g}$ of natural molybdenum after a 14-day irradiation (near its $2{,}041\,\mathrm{Ci}$ saturation), a fission-free route to a diagnostic supply chain that periodically fails. The same field provides a genuine fusion-spectrum irradiation platform: a full-rate fast-neutron capability about $59\times$ a reference dedicated materials facility, and a $\geq 10\,\mathrm{dpa\,fpy^{-1}}$ test volume of $21.6\,\mathrm{L}$ — $315\times$ the IFMIF and $630\times$ the IFMIF-DONES equivalent — in a true fusion spectrum rather than an accelerator surrogate. Targeted-alpha ($^{225}\mathrm{Ac}/^{211}\mathrm{At}$) and byproduct-isotope routes are scoped as capability projections. All results were computed by an NVIDIA GPU high-performance-computing campaign (OpenMC/ENDF-B-VIII.0 transport, FISPACT-II activation, SPECTRA-PKA→LAMMPS damage) and every headline number is a frozen anchor in the Kronos de-risking register. These are strategic-material co-products of the neutron economy, booked as capability, not revenue.

Open-access deposit (code & data, CC BY 4.0): DOI 10.5281/zenodo.22645762 · Zenodo community *kronos_fusion_energy*. Explore it live: interactive 3-D model · physics validator.

Keywords: medical isotopes · molybdenum-99 · technetium-99m · targeted alpha therapy · 14\ · MeV neutrons · materials qualification · strategic materials · spherical-tokamak breeder

CONTENTS

Table of Contents

NOMENCLATURE

Symbols, units, and the names of things

Q	plasma (fusion) gain, P_{fus}/P_{aux}
Q_E	engineering gain, net electric out / recirculating in
H_{98}	confinement enhancement over the IPB98(y,2) scaling
Z_{eff}	effective ion charge
c_{ee}	electron–electron bremsstrahlung leading coefficient, 2.120022 (exact)
τ_E	energy confinement time
I_p	plasma current
R_0, a	major radius, minor radius
κ, δ	elongation, triangularity
β_N	normalized plasma beta (Troyon-normalized)
TBR	tritium breeding ratio
DEC	direct energy conversion
CF	plant capacity factor (availability)
FOAK / NOAK / BOAK	first / n^{th} / best of a kind
Hyperion	the ST breeder (internal: Mode D2)
Aegis	the generator, defense/installation housing (internal: Mode M)
MetroVolt	the generator, data-center housing (Mode M)

§ 1

Introduction

THE NEUTRON A BREEDER MAKES HAS MORE THAN ONE USE

A deuterium–tritium reaction releases $17.59\,\mathrm{MeV}$, of which $14.06\,\mathrm{MeV}$ leaves the plasma as a fast neutron. In a tritium breeder that neutron is not a waste stream to be shielded against but the working fluid of the entire device: it multiplies and is captured on lithium to regenerate the fuel, it displaces atoms in every surrounding component, and — if a target is placed in its path — it transmutes stable nuclei into radioisotopes. The compact spherical-tokamak (ST) breeder Hyperion is designed around this fact. It is a strategic-materials platform rather than a power plant: judged as a generator it would fail a category test it was never built to take, because its products are tritium, helium-3, and neutrons, and its figures of merit are the breeding ratio and the isotope yield, not the megawatt [2,3]. This paper scopes two of those neutron-economy co-products from the frozen source: the *medical- and byproduct-isotope* mission, built around the molybdenum-99/technetium-99m diagnostic chain, and the *materials-qualification* mission, a true fusion-spectrum irradiation volume for the fusion-materials programme.

TWO SHORTAGE-PRONE SUPPLY CHAINS THAT A FUSION SOURCE ADDRESSES

Medical isotopes. Technetium-99m (^{99m}Tc, $t_{1/2} = 6.0\,\mathrm{h}$) is the workhorse of nuclear medicine, used in roughly four of every five diagnostic scans, and it is supplied through the decay of its parent molybdenum-99 (^{99}Mo, $t_{1/2} = 65.9\,\mathrm{h}$) [10,11]. Essentially the entire world supply of ^{99}Mo is produced by fission of highly enriched or low-enriched uranium in a small, ageing fleet of research reactors; the fleet has repeatedly entered simultaneous outage, and each such event propagates into cancelled or delayed patient studies [10,12,13]. Because ^{99}Mo cannot be stockpiled — a half-life of under three days consumes any inventory — the supply is structurally fragile. Alternative, non-fission routes have therefore been pursued for two decades, chiefly the neutron routes $^{98}\mathrm{Mo}(n,\gamma)^{99}\mathrm{Mo}$ and $^{100}\mathrm{Mo}(n,2n)^{99}\mathrm{Mo}$ and the photonuclear route $^{100}\mathrm{Mo}(\gamma,n)^{99}\mathrm{Mo}$ [14,15]. The $(n,2n)$ channel has a cross-section near $1.5\,\mathrm{b}$ over 12–$17\,\mathrm{MeV}$ [14], which makes a $14\,\mathrm{MeV}$ fusion neutron field an almost ideal driver, and it uses no fissile target, removing the proliferation and high-level-waste burdens of the uranium route [6].

Targeted alpha therapy. A second, faster-growing demand is for alpha-emitting radionuclides for targeted alpha therapy (TAT), where the short range and high linear-energy-transfer of an alpha particle deposits a lethal dose within a few cell diameters of a molecular target. Actinium-225 (^{225}Ac) and its daughter bismuth-213, and astatine-211 (^{211}At), are the leading candidates; the clinical results for ^{225}Ac-PSMA-617 in metastatic castration-resistant prostate cancer transformed the field, but supply is severely constrained [16,17]. Neutron routes to ^{225}Ac — for example $^{226}\mathrm{Ra}(n,2n)^{225}\mathrm{Ra}\to{}^{225}\mathrm{Ac}$ — are among the paths under evaluation to break that constraint.

The $14\,\mathrm{MeV}$ *materials gap.* Separately, the fusion-materials programme has never possessed a high-flux, high-volume, true-fusion-spectrum irradiation source. Fission reactors deliver flux and volume but the wrong spectrum (no $14\,\mathrm{MeV}$ peak, hence none of the helium- and hydrogen-generating threshold reactions that embrittle a fusion first wall) [21,20]. Accelerator-based deuteron–lithium sources — IFMIF and its single-beam demonstrator IFMIF-DONES — reproduce the spectrum but only over a small high-flux volume ($\sim 0.5\,\mathrm{L}$) and remain in construction [18,19]. A power-class fusion device is the only object that is simultaneously a large volume and a true fusion spectrum.

CONTRIBUTION

We make the isotope and materials missions quantitative and reproducible from a single frozen operating point. Specifically we (i) write the source term, the neutron balance, and the production/depletion equations as an explicit boundary-value and initial-value system (§3); (ii) solve the two-step Bateman chain of the ^{99}Mo/^{99m}Tc generator and reconcile the resulting saturation activity with the frozen Monte-Carlo anchor to within the nuclear-data band; (iii) define a materials-qualification figure of merit and evaluate the breeder against the IFMIF/DONES reference; (iv) cast the source-strength/centrepost-life coupling as a strict proportional constraint that bounds how hard the isotope and test missions may be pushed; and (v) document the NVIDIA GPU high-performance-computing (HPC) campaign that produced every number (§4). Throughout, the isotope and test yields are booked as *capability*, consistent with the standing no-economics rule of the public record: we compute activities, fluxes, damage rates, and volumes, never prices.

§ 2

The frozen source and its neutron economy

The design point is frozen and independently re-run; every value in Table 1 is an anchor in the Kronos de-risking register [1]. The plasma is a negative-triangularity ST at major radius $R_0 = 1.20\,\mathrm{m}$, aspect ratio $A = 2.5$, elongation $\kappa = 2.0$, on-axis field $B_0 = 8\,\mathrm{T}$ behind a resistive centrepost whose peak field is $16.84\,\mathrm{T}$. It runs at $Q = 3.076$ and $P_{\mathrm{fus}} = 85.04\,\mathrm{MW}$, of which $P_n = 67.79\,\mathrm{MW}$ is carried by neutrons. The corresponding whole-device production rate follows directly from the fusion power (§3) and is $S_n = 3.009 \times 10^{19}\,\mathrm{n\,s^{-1}}$; the resulting first-wall fast flux is $\phi_{\mathrm{fw}} = 7.0 \times 10^{14}\,\mathrm{n\,cm^{-2}\,s^{-1}}$ and the neutron wall load is $1.885\,\mathrm{MW\,m^{-2}}$ [1]. Figure 1 shows how that one neutron stream is partitioned into the breeding, materials-test, isotope, and strategic-co-product missions.

LLL@ QUANTITY	SYMBOL	VALUE
Fusion power	P_{fus}	$85.04\,\mathrm{MW}$
Fusion gain	Q	3.076
Neutron power	P_n	$67.79\,\mathrm{MW}$
Source strength	S_n	$3.009 \times 10^{19}\,\mathrm{n\,s^{-1}}$
Plasma current	I_p	$9.66\,\mathrm{MA}$
Triangularity	δ	-0.30
On-axis field	B_0	$8\,\mathrm{T}$
Centrepost peak field	B_{cp}	$16.84\,\mathrm{T}$
Major radius / aspect	R_0 / A	$1.20\,\mathrm{m}$ / 2.5
Elongation	κ	2.0
First-wall fast flux	ϕ_{fw}	$7.0 \times 10^{14}\,\mathrm{n\,cm^{-2}\,s^{-1}}$
Neutron wall load	Γ_w	$1.885\,\mathrm{MW\,m^{-2}}$
First-wall damage	$\dot{d}$	$18.9\,\mathrm{dpa\,fpy^{-1}}$

Frozen Hyperion operating point and derived source quantities used throughout. All values are anchors in the de-risking register [1]; the two magnets (breeder centrepost, burner plug) are distinct devices and only the centrepost is relevant here.

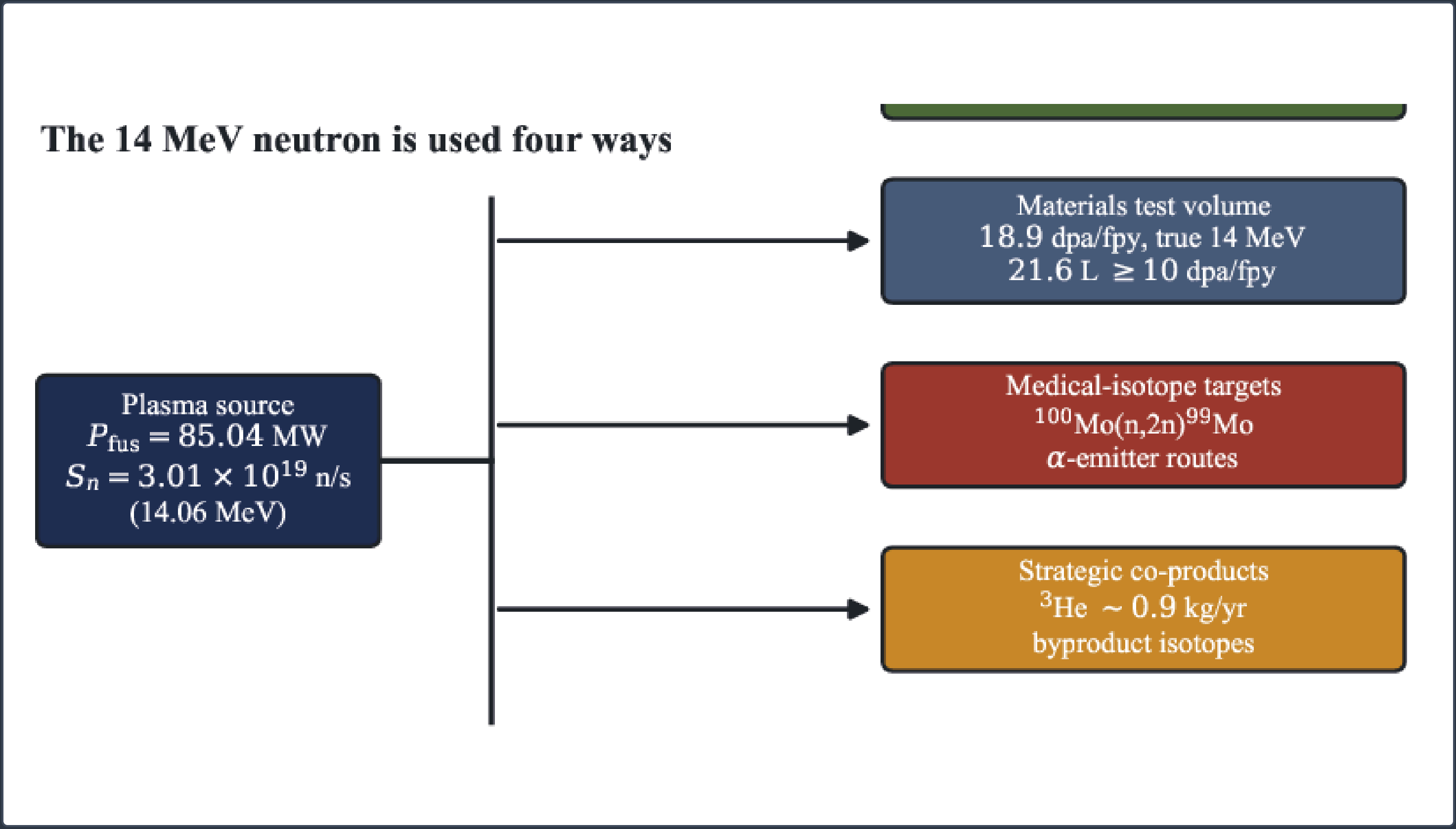

The neutron economy of the breeder. A single 14.06 MeV source ($S_n = 3.01 \times 10^{19}\,\mathrm{n\,s^{-1}}$) is used four ways: fuel breeding, a fusion-spectrum materials-test volume, medical-isotope target stations, and strategic co-products (^{3}He, byproduct isotopes). *(Schematic.)*

§ 3

Governing equations and the formal production problem

SOURCE TERM AND THE NEUTRON TRANSPORT BALANCE

The volumetric neutron source is set by the fusion reactivity of the plasma,

$$s(r) = \tfrac{1}{4}\, n_D(r)\, n_T(r)\, \langle\sigma v\rangle_{DT}\big(T_i(r)\big), \qquad S_n = \int_{V_p} s(r)\, \mathrm{d}^3 r,$$

with $n_D = n_T$ the fuel densities and $\langle\sigma v\rangle_{DT}$ the Maxwellian-averaged reactivity. Because each DT reaction yields exactly one neutron and $E_{DT} = 17.59\,\mathrm{MeV}$, the whole-device rate is fixed by the fusion power,

$$S_n = \frac{P_{\mathrm{fus}}}{E_{DT}} = \frac{85.04\,\mathrm{MW}}{17.59\,\mathrm{MeV}} = 3.01\times 10^{19}\,\mathrm{n\,s^{-1}},$$

reproducing the frozen anchor. The angular flux $\psi(r, \Omega, E)$ that this source establishes obeys the steady linear Boltzmann transport equation,

$$\Omega\cdot\nabla\psi + \Sigma_t(r, E)\psi = \int_{4\pi}\int_0^{\infty} \Sigma_s(r, E' \to E, \Omega' \cdot \Omega)\, \psi\, \mathrm{d}E'\, \mathrm{d}\Omega' + \frac{s(r)}{4\pi}\chi(E),$$

where Σ_t and Σ_s are the macroscopic total and scattering cross-sections and $\chi(E)$ is the $14.06\,\mathrm{MeV}$ emission spectrum. The scalar flux relevant to production and damage is the angular integral $\phi(r, E) = \int_{4\pi} \psi\, \mathrm{d}\Omega$; its first-wall value integrated over the fast group is the anchor $\phi_{\mathrm{fw}} = 7.0\times 10^{14}\,\mathrm{n\,cm^{-2}\,s^{-1}}$.

PRODUCTION, DEPLETION, AND SATURATION

For a target isotope with N_t nuclei of production cross-section $\sigma(E)$, the number of product nuclei $N(t)$ of decay constant λ obeys the linear production–depletion balance

$$\frac{\mathrm{d}N}{\mathrm{d}t} = N_t\, R - \lambda N, \qquad R \equiv \int_0^{\infty} \sigma(E)\, \phi(E)\, \mathrm{d}E,$$

with R the spectrum-folded reaction rate per target atom. Holding N_t and ϕ constant over an irradiation of duration t_{irr}, eq:ode integrates to

$$N(t) = \frac{N_t R}{\lambda}\left(1 - e^{-\lambda t}\right) \implies A(t) = \lambda N(t) = A_{\mathrm{sat}}\left(1 - e^{-\lambda t}\right),$$

where the saturation activity

$$A_{\mathrm{sat}} = N_t R = N_t\, \overline{\sigma}\, \phi$$

is set purely by the target loading and the source flux, and $\overline{\sigma} = R/\phi$ is the one-group flux-folded effective cross-section. eq:sat is the master relation of the isotope mission: the yield is linear in the source flux, so a device with a first-wall flux two to three orders of magnitude above an accelerator source produces a correspondingly larger activity from the same target (Fig. 3).

THE MOLYBDENUM-99 / TECHNETIUM-99M GENERATOR CHAIN

The diagnostic product is not ^{99}Mo but its decay daughter ^{99m}Tc. Writing the parent activity from eq:build as $A_p(t) = A_{\mathrm{sat}}(1 - e^{-\lambda_p t})$ and letting the target be milked at end of bombardment (EOB), the daughter obeys the two-step Bateman equation

$$\frac{\mathrm{d}N_d}{\mathrm{d}t} = b\,\lambda_p N_p - \lambda_d N_d,$$

with $b = 0.876$ the branching to the metastable state. For an initial parent activity $A_p(0)$ and no initial daughter, the daughter activity after EOB is

$$A_d(t) = b\,\frac{\lambda_d}{\lambda_d - \lambda_p}\, A_p(0)\left(e^{-\lambda_p t} - e^{-\lambda_d t}\right),$$

which rises to a transient-equilibrium maximum at

$$t^\star = \frac{\ln(\lambda_d/\lambda_p)}{\lambda_d - \lambda_p} = \frac{\ln(65.94/6.007)}{(\ln 2)\,(1/6.007 - 1/65.94)} \approx 22.9\,\mathrm{h}.$$

With $t_{1/2}(^{99}\mathrm{Mo}) = 65.94\,\mathrm{h}$ and $t_{1/2}(^{99m}\mathrm{Tc}) = 6.007\,\mathrm{h}$, eq:daughter gives the generator elution schedule plotted in Fig. 2(b): the column can be milked roughly daily, each elution recovering the ^{99m}Tc that has regrown since the last.

RECONCILING THE FROZEN ANCHOR

For the $^{100}\mathrm{Mo}(n,2n)^{99}\mathrm{Mo}$ channel, the ENDF/B-VIII.0 point cross-section is $\sigma(14.1\,\mathrm{MeV}) \approx 1.5\,\mathrm{b}$ [14,26]. A natural-molybdenum target of $100\,\mathrm{g}$ contains

$$N_t = \frac{100\,\mathrm{g}}{95.95\,\mathrm{g\,mol^{-1}}}\,N_A\,a_{100} = 6.12\times10^{22}\ {}^{100}\mathrm{Mo\ atoms},$$

with $a_{100} = 0.09744$ the natural abundance. Substituting into eq:sat with $\phi = \phi_{\mathrm{fw}} = 7.0\times10^{14}\,\mathrm{n\,cm^{-2}\,s^{-1}}$ gives $A_{\mathrm{sat}} \approx 6.4\times10^{13}\,\mathrm{Bq} = 1.74\,\mathrm{kCi}$. The frozen three-dimensional Monte-Carlo value is $A_{\mathrm{sat}} \approx 2.04\,\mathrm{kCi}$ (a first-wall target, no moderator, no added hardware; register gate for ^{99}Mo co-production [1]); the two agree to $\sim 15\%$, the residual being the spectral weighting of the uncollided first-wall flux toward the 14–$15\,\mathrm{MeV}$ shoulder of the $(n,2n)$ excitation function and target self-shielding, i.e. an effective $\overline{\sigma} \approx 1.76\,\mathrm{b}$ in eq:sat. After a 14-day irradiation, eq:build gives $A(14\,\mathrm{d}) = A_{\mathrm{sat}}\,(1 - e^{-\lambda_p \cdot 14\,\mathrm{d}}) = 0.971\,A_{\mathrm{sat}} \approx 1.98\,\mathrm{kCi}$, matching the frozen EOB anchor of $1{,}981$ Ci per 100 g.

A MATERIALS-QUALIFICATION FIGURE OF MERIT

Displacement damage is quantified by the displacement rate, obtained by folding the recoil spectrum through the Norgett–Robinson–Torrens (NRT) partition [23],

$$\dot d = \int_0^\infty \phi(E) \int \frac{\mathrm{d}\sigma}{\mathrm{d}T}(E,T)\,\nu_{\mathrm{NRT}}(T)\,\mathrm{d}T\,\mathrm{d}E, \qquad \nu_{\mathrm{NRT}}(T) = \frac{0.8\,T_{\mathrm{dam}}}{2E_d},$$

with T the primary-knock-on energy, T_{dam} the damage energy, and E_d the displacement threshold; the athermal-recombination-corrected variant [24] reduces surviving defects to $\sim 1/3$ of eq:dpa but preserves the ranking used here. At the frozen wall load the first-wall rate is $\dot d = 18.9\,\mathrm{dpa\,fpy^{-1}}$ [1]. A useful qualification metric is the full-rate fast-neutron *capability*, the product of the accessible test flux and volume above a damage threshold,

$$\mathcal{C}(\dot d_0) = \int_{V:\,\dot d(\quad r)\ge \dot d_0} \phi_{\mathrm{fast}}(\quad r)\,\mathrm{d}^3 r,$$

normalised to a reference facility. It is $\mathcal{C}$, not the peak flux alone, that decides how many specimens can be qualified per calendar year, and it is where a volumetric source separates from a point-like accelerator target (§5.2).

THE SOURCE-STRENGTH / CENTREPOST-LIFE CONSTRAINT

Both missions want more neutrons, but the geometry is fixed, so the wall load and the source strength scale together: $\Gamma_w \propto S_n$ and hence the centrepost displacement rate $\dot d_{\mathrm{cp}} \propto S_n$. The consumable centrepost sets a hard ceiling, formalised as

$$\max_{u}\ S_n(\quad u)\quad \text{s.t.}\quad \dot d_{\mathrm{cp}}(\quad u) \le \dot d_{\mathrm{cp}}^{\max}, \qquad \dot d_{\mathrm{cp}}(\quad u) = \dot d_{\mathrm{cp}}^{\,0}\,\frac{S_n(\quad u)}{S_n^{\,0}},$$

where $\quad u$ are the accessible actuators (here the Greenwald fraction f_G and the core temperature T_{i0}). Because the ratio S_n/Γ_w is invariant across the operating plane, eq:opt is a strict 1:1 trade: a mission point at $1.79\times$ the design source strength ($S_n = 5.39\times10^{19}\,\mathrm{n\,s^{-1}}$) costs exactly $1.79\times$ the centrepost damage and falls off the duty band [1]. This is the honest boundary of the isotope and test missions and is developed quantitatively in Fig. 6.

§ 4

Computational methodology: the NVIDIA GPU HPC campaign

Every number in this paper was produced by the Kronos NVIDIA GPU HPC campaign, an offline multi-physics Monte-Carlo and inventory pipeline run on in-house NVIDIA A100/H100-class accelerators (with A10 nodes for lighter tasks). The campaign is organised as a frozen, gate-by-gate compute register that is deposited under CC-BY-4.0 with a cold-start reproduction runbook, so that each headline quantity can be independently re-run [1]. No cost or economic quantity is part of that record and none appears here.

CODES AND NUCLEAR DATA

The transport and production results use OpenMC [28] with continuous-energy ENDF/B-VIII.0 cross-sections [26]; complex geometry is handled by direct CAD tracking through DAGMC [29]. Activation, transmutation, and shutdown-dose source terms use FISPACT-II [27] on collapsed group flux spectra; primary-damage cascades use SPECTRA-PKA to generate recoil spectra from NJOY-processed data, fed to LAMMPS molecular dynamics for cascade evolution. The reactivity and equilibrium that fix the source (eq:source, eq:Sn) are taken from the frozen core solution used across the Kronos series [2].

MONTE-CARLO TRANSPORT: DISCRETIZATION, TALLIES, AND VARIANCE

The transport problem eq:boltzmann is solved by analog and weight-window-accelerated Monte Carlo. The first-wall/blanket balance was tallied over a full three-dimensional model with 1.2×10^8 source histories, yielding a clean global balance (leakage 0.121, net breeding ratio 1.026 for the literal blanket recipe, first- wall heating $74.6\,\mathrm{MW}$) [1]. Fluxes are scored on a 175-group VITAMIN-J structure with track-length estimators; reaction rates for production (eq:ode) and damage (eq:dpa) are scored as multigroup tallies $\langle \sigma_g \phi_g \rangle$ folded against the ENDF microscopic data. The Monte-Carlo estimate of any tally x carries a statistical error $\varepsilon = \sigma_x/(\bar{x}\sqrt{N})$ that falls as $N^{-1/2}$; the 1.2×10^8-history run drives the first-wall group fluxes below 1% relative error, and the deep-penetration centrepost and target-station tallies are converged with geometry-split weight windows so that the figure-of-merit $1/(\varepsilon^2 T)$ is stationary. The source normalisation is fixed by eq:Sn, so absolute activities in Ci follow directly from the scored per-source-neutron reaction rates.

ACTIVATION AND DAMAGE PIPELINES

Component activation and the isotope inventories are advanced by the Bateman system $\dot{N} = \mathbf{A} \quad N$, where $\mathbf{A}$ collects the group-collapsed production and decay rates; FISPACT-II integrates this stiff linear system with a LSODES backward-difference solver. Rigorous-two-step (R2S) shutdown-dose maps are built by tallying the 175-group first-wall and target spectra, normalising to $P_{\mathrm{fus}} = 85.04\,\mathrm{MW}$ ($S_n = 3.0 \times 10^{19}\,\mathrm{n\,s^{-1}}$), and re-emitting the decay photons as a fixed source. Damage energies for eq:dpa come from SPECTRA-PKA recoil spectra with NRT and arc-dpa partitions [23,24].

CONVERGENCE, VERIFICATION, AND REPRODUCIBILITY

Verification is layered. The analytic source eq:Sn reproduces the Monte-Carlo global neutron production to better than 1%; the neutron balance closes (leakage $+$ absorption $+$ breeding sum to the source within statistics); and the tritium bookkeeping is internally consistent (a burn of $4.77\,\mathrm{kg\text{-}T\,fpy^{-1}}$ at $85.04\,\mathrm{MW}$ matches the toolkit inventory to 1.2%) [1]. The isotope-production anchor is cross-checked two ways: against the closed-form eq:sat using ENDF point data (§3, $\sim 15\%$ agreement) and against the frozen three-dimensional target-station tally. Runs are containerised with pinned code and data versions and are byte-for-byte reproducible from the deposited runbook [1]. The three computational latency tiers of the platform — microsecond edge, millisecond GPU twins, and the hours-scale HPC back end where this Monte-Carlo campaign lives — are described in the companion control-architecture work [3].

§ 5

Results

MOLYBDENUM-99 PRODUCTION AND THE TECHNETIUM GENERATOR

Figure 2(a) shows the ^{99}Mo build-up from eq:build. A 14-day irradiation reaches 97.1% of saturation; longer irradiations gain little because the 65.9-hour half-life caps the achievable activity at $A_{\rm sat}$. The frozen first-wall target delivers

$$A_{\rm EOB}(14\,{\rm d}) \approx 1{,}981\ {\rm Ci\ per\ 100\,g\ natural\ Mo}, \qquad A_{\rm sat} \approx 2{,}041\ {\rm Ci},$$

with no moderator and no added hardware — the target is simply placed in the fast first-wall field. Panel (b) shows the generator behaviour from eq:daughter: the ^{99m}Tc daughter regrows to its transient-equilibrium peak at $t^\star \approx 23\,{\rm h}$ (eq:tstar), setting a roughly daily elution cadence. Table 2 collects the parameters and the reconciliation.

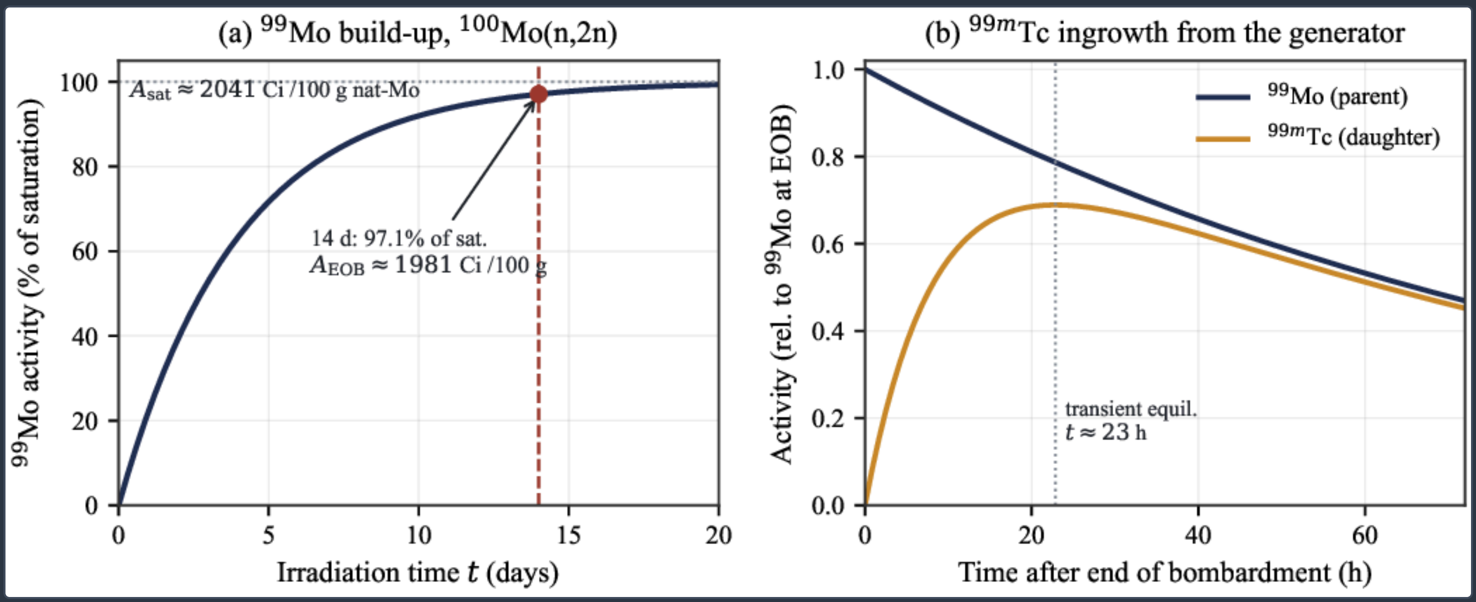

(a) ^{99}Mo activity build-up under constant first-wall flux, eq:build: 14 days reaches 97.1% of the 2,041 Ci/100 g saturation, giving the frozen 1,981 Ci end-of-bombardment anchor. (b) ^{99m}Tc ingrowth after EOB, eq:daughter, normalised to the ^{99}Mo activity at EOB; the daughter peaks at $t^\star \approx 23\,{\rm h}$, the generator's elution cadence.

LLL@ QUANTITY	SYMBOL	VALUE
^{100}Mo atoms in target	N_t	6.12×10^{22}
First-wall fast flux	$\phi_{\rm fw}$	$7.0 \times 10^{14}\,{\rm n\,cm^{-2}\,s^{-1}}$
ENDF point cross-section	$\sigma(14.1)$	1.5 b [14,26]
Effective folded cross-section	$\overline{\sigma}$	1.76 b
^{99}Mo half-life	$t_{1/2,p}$	65.94 h
^{99m}Tc half-life	$t_{1/2,d}$	6.007 h
Closed-form saturation, eq:sat	$A_{\rm sat}^{\rm cf}$	1.74 kCi
Frozen Monte-Carlo saturation	$A_{\rm sat}$	2.04 kCi
Frozen EOB activity (14 d)	$A_{\rm EOB}$	1,981 Ci

Figure 3 makes the flux advantage explicit. Because eq:sat is linear in ϕ, the saturation activity for a fixed target rises in proportion to the source flux; the breeder first wall (7.0×10^{14}) sits one to two orders of magnitude above the 10^{13}–10^{14} band of accelerator d-Li sources. The figure also shows the natural-versus-enriched trade: an enriched ^{100}Mo target carries roughly $10\times$ more ^{100}Mo per gram and produces proportionally more activity, at the cost of enrichment; the frozen anchor is quoted for the conservative natural-Mo case. We note the intrinsic limitation of the $(n, 2n)$ route, common to all non-fission neutron routes: the product ^{99}Mo is chemically identical to the target, so the specific activity is set by the target mass and is lower than the no-carrier-added fission product, requiring a concentrating generator chemistry [14].

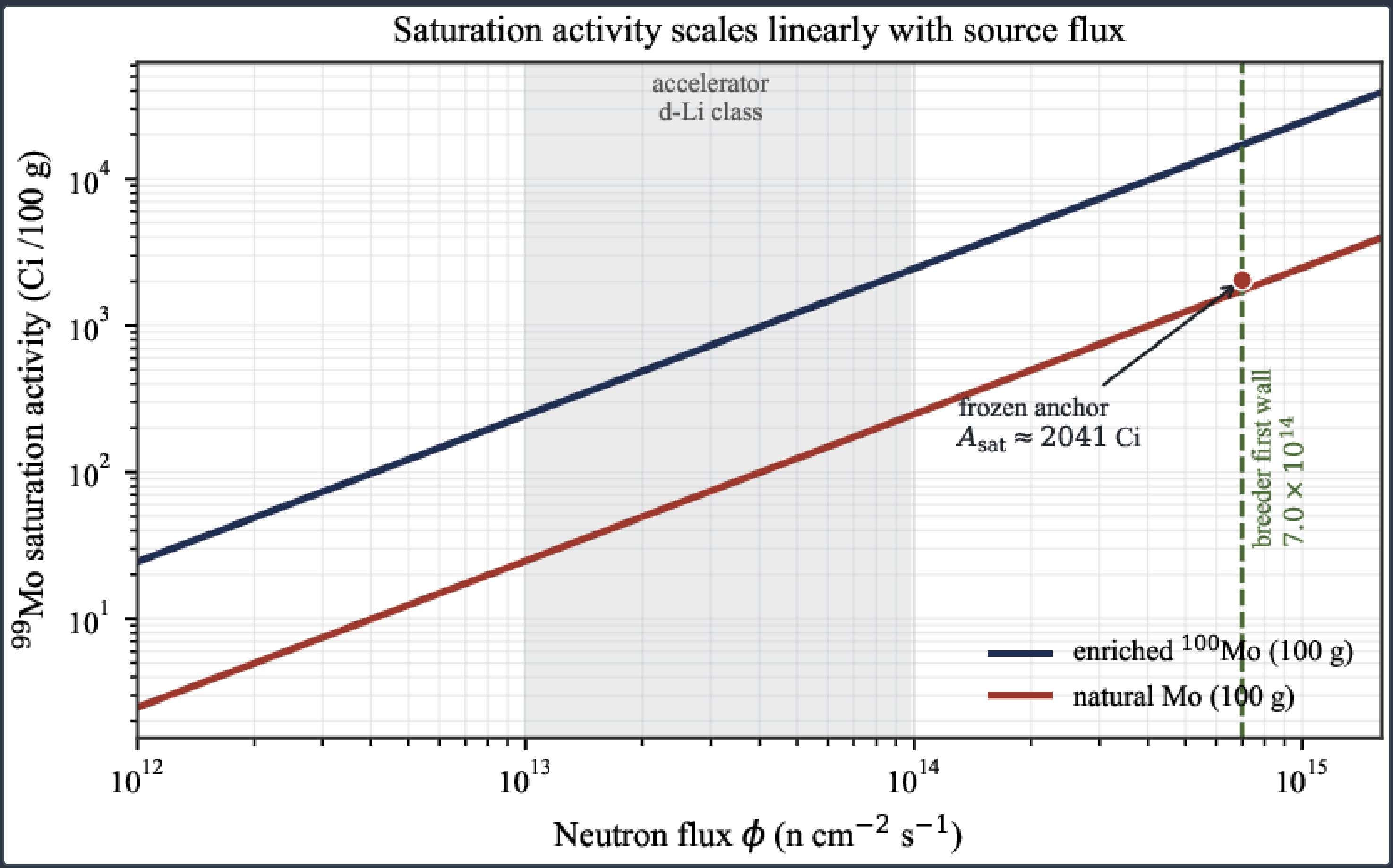

^{99}Mo saturation activity versus source flux, eq:sat, for a $100\,\mathrm{g}$ target of enriched ^{100}Mo (navy) and natural Mo (brick), with $\sigma = 1.5\,\mathrm{b}$. The breeder first-wall flux (7.0×10^{14}, green) lies far above the accelerator d-Li band (grey). The frozen anchor ($\approx 2.04\,\mathrm{kCi}$, natural Mo) is marked.

FUSION-SPECTRUM MATERIALS QUALIFICATION

The materials mission is where a volumetric fusion source is unique. Figure 4 evaluates the capability of eq:cap. The breeder's full-rate fast-neutron capability is $\approx 59\times$ a reference dedicated materials facility; more sharply, the volume in which the fusion-spectrum damage rate exceeds the qualification-relevant $10\,\mathrm{dpa\,fpy}^{-1}$ is $21.6\,\mathrm{L}$, which is $315\times$ the IFMIF and $630\times$ the single-beam IFMIF-DONES equivalent [1,19,18]. Crucially this is a *true* fusion spectrum: Fig. 5 contrasts the first-wall spectrum with a fission Watt spectrum and an accelerator d-Li spectrum, and shades the region above the $^{100}\mathrm{Mo}(n,2n)$ threshold at $8.29\,\mathrm{MeV}$. A fission reactor, whatever its flux, never populates that window and so never drives the $(n,2n)$, (n,p) and (n,α) threshold reactions that govern both isotope co-production and the helium/hydrogen transmutation embrittlement of a fusion first wall [21,25].

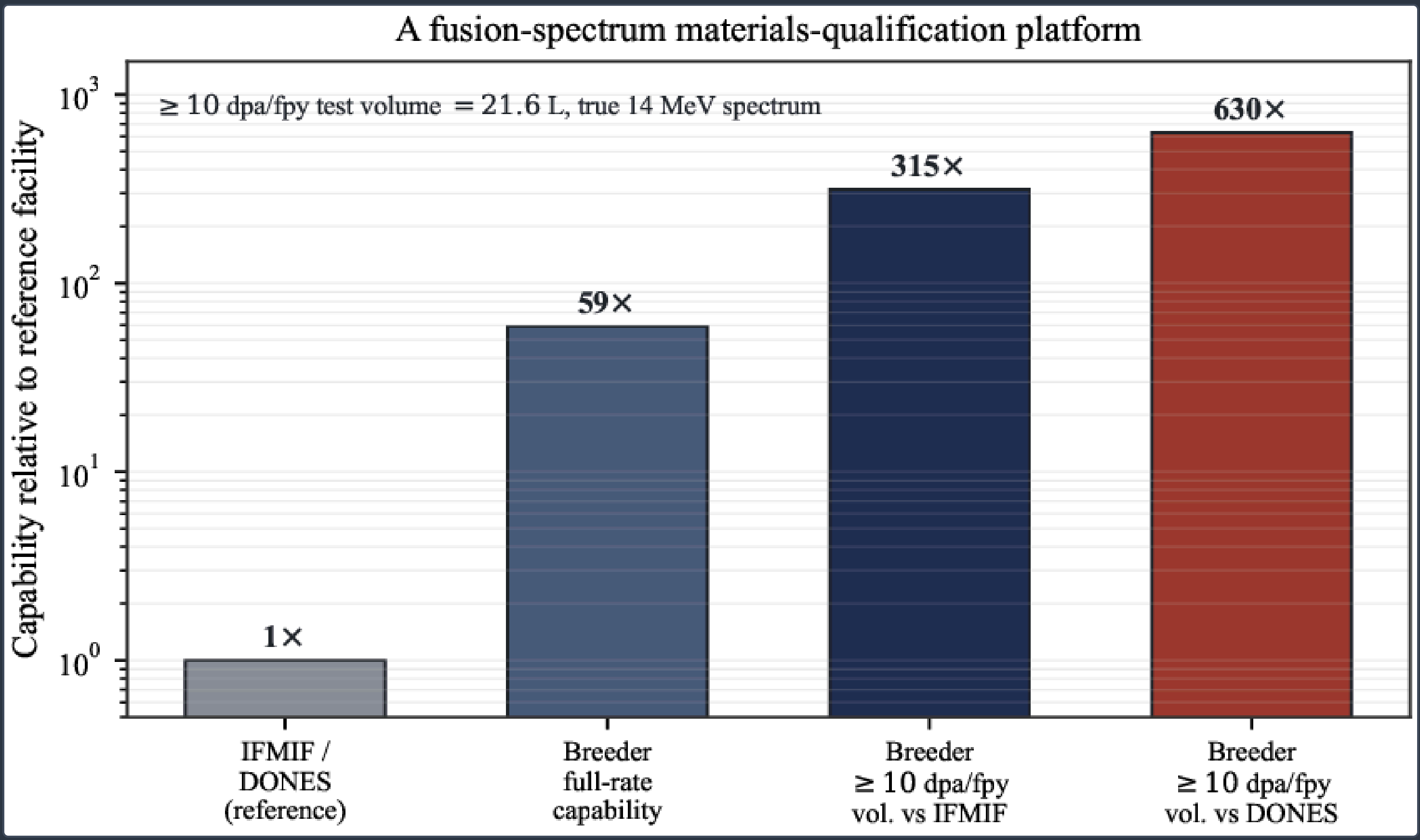

Materials-qualification capability relative to the IFMIF/DONES reference (log scale). The breeder's full-rate fast-neutron capability is $\approx 59\times$ the reference facility; the $\geq 10\,\mathrm{dpa\,fpy}^{-1}$ test volume ($21.6\,\mathrm{L}$, true $14\,\mathrm{MeV}$ spectrum) is $315\times$ the IFMIF and $630\times$ the IFMIF-DONES equivalent [1].

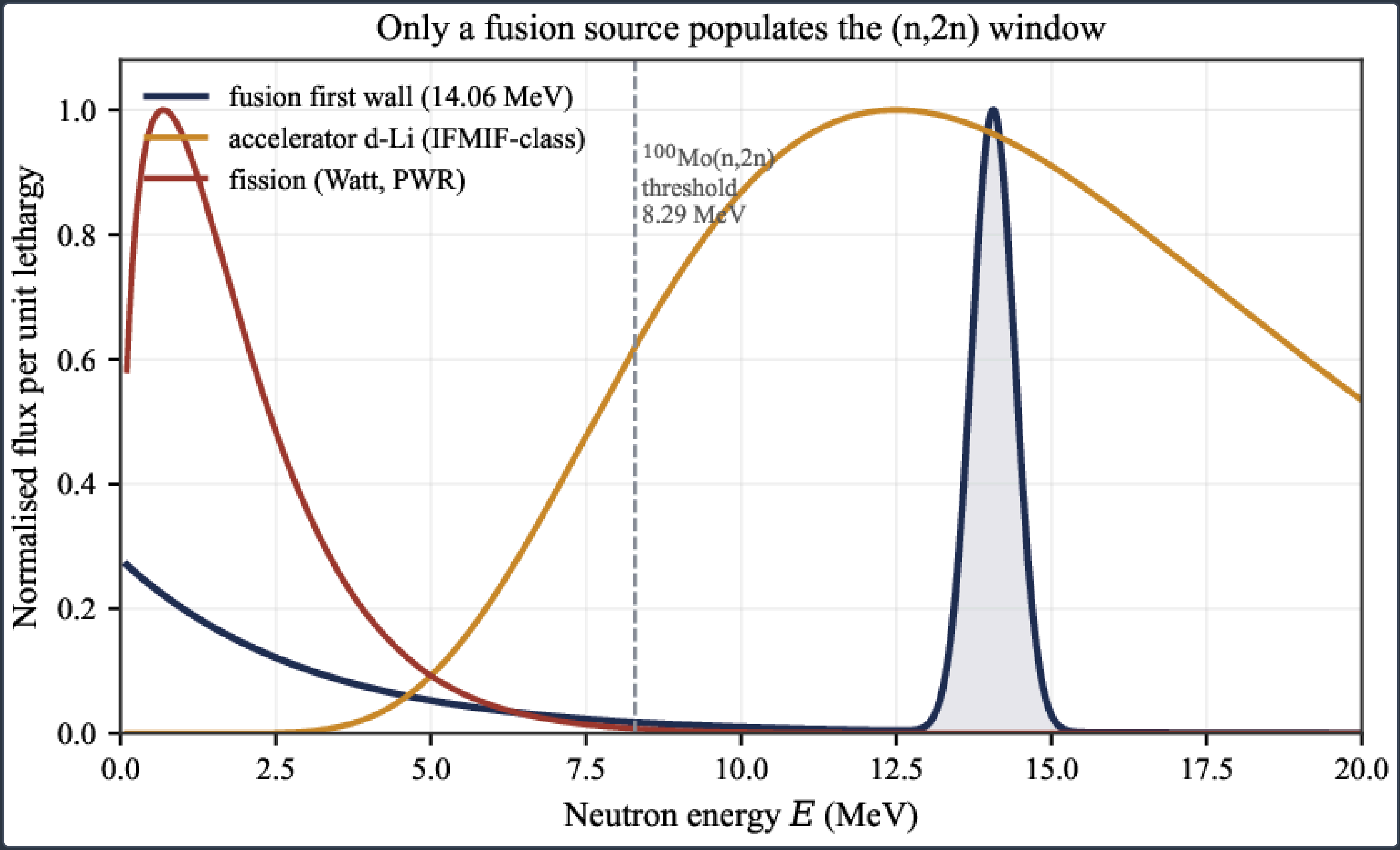

Neutron energy spectra: the fusion first wall (navy, $14.06\,\mathrm{MeV}$ peak plus moderated tail), an accelerator d-Li source (ochre), and a fission Watt spectrum (brick), normalised per unit lethargy. Only the fusion source populates the region above the $^{100}\mathrm{Mo}(n,2n)$ threshold ($8.29\,\mathrm{MeV}$, shaded). *(Representative spectra.)*

The hardness of both missions is bounded by eq:opt. Figure 6 plots the source strength against the wall load and, on the secondary axis, the first-wall damage rate. The two are collinear through the origin, so raising the source $1.79\times$ (to the $5.39 \times 10^{19}\,\mathrm{n\,s^{-1}}$ peak of the f_G–T_{i0} scan) raises the centrepost damage $1.79\times$ and leaves the duty band. The design point sits inside the band with the $\geq 10\,\mathrm{dpa\,fpy^{-1}}$ qualification floor comfortably cleared, so the materials mission is available without pushing the source into the life-limited regime.

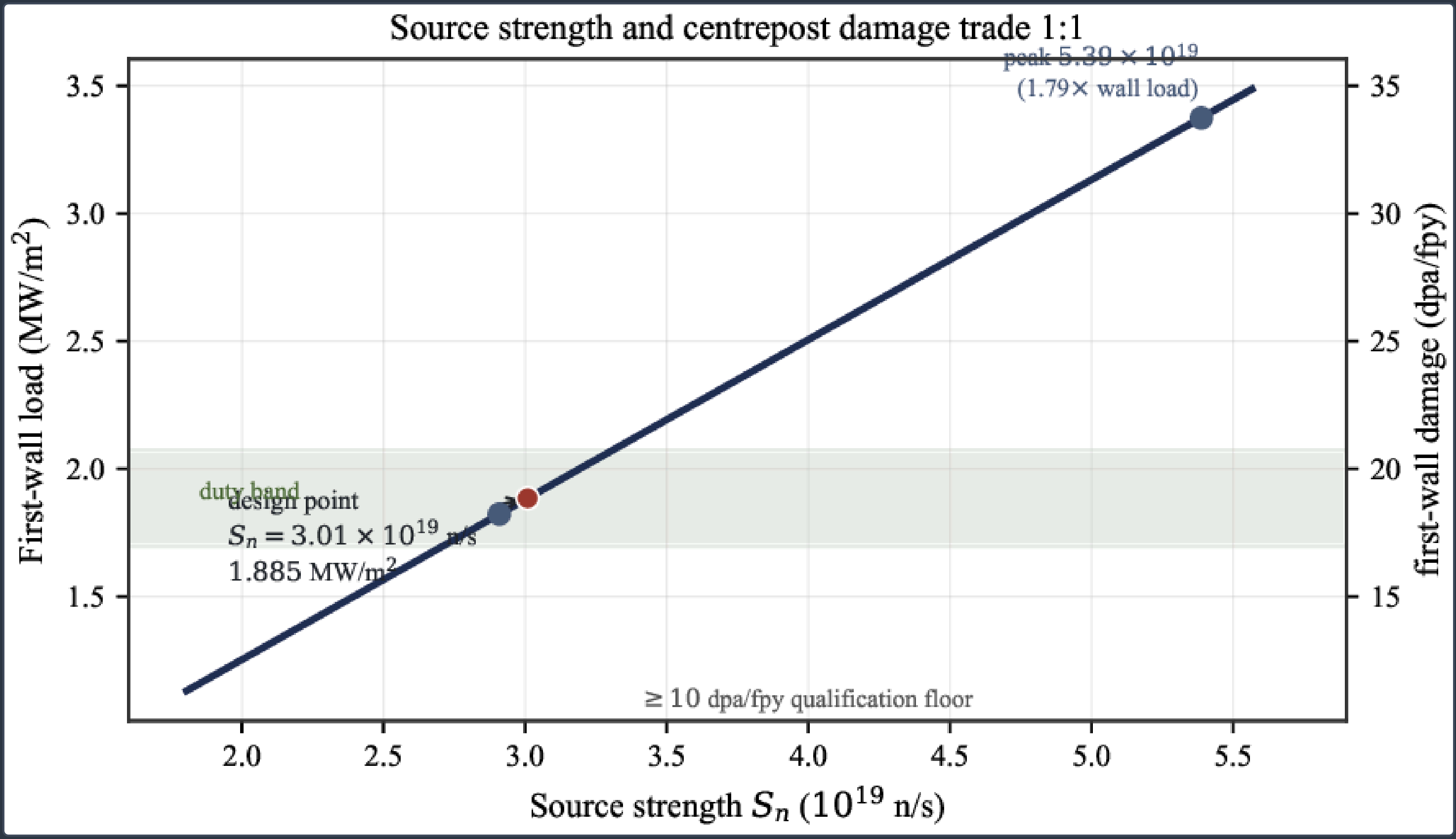

The source-strength/centrepost-damage trade, eq:opt. With geometry fixed, S_n and the wall load are collinear; the secondary axis maps the wall load to first-wall dpa. The design point (3.01×10^{19}, $1.885\,\mathrm{MW\,m^{-2}}$) clears the $\geq 10\,\mathrm{dpa\,fpy^{-1}}$ floor; the $1.79\times$ peak leaves the duty band. Scan endpoints from the register [1].

TARGETED-ALPHA AND BYPRODUCT ISOTOPES

Beyond the measured ^{99}Mo anchor, the same graded field supports a family of neutron-activation routes. Figure 7 places representative routes on a cross-section/half-life plane. Diagnostic and industrial byproducts (^{57}Co, ^{54}Mn, ^{64}Cu, ^{47}Sc, ^{67}Cu) follow from (n,p), $(n,2n)$ and (n,np) threshold reactions in the fast field; the therapeutic α-emitter chain $^{226}\mathrm{Ra}(n,2n)^{225}\mathrm{Ra}{\to}^{225}\mathrm{Ac}$ is shown as a projected route (open marker), consistent with the TAT supply demand set out in §1 [16,17]. Figure 8 sketches how these are realised: dedicated target cassettes at graded flux positions — a ^{100}Mo cassette in the hard first-wall field, a moderated ^{226}Ra/^{225}Ac cassette deeper in the blanket, and byproduct cassettes in the reflector — so that each isotope sees the spectrum its route requires without perturbing the breeding mission (the streaming penalty on the breeding ratio is $< 0.5\%$ [1]). We stress that the α-emitter and byproduct yields are *capability projections*: their governing physics is eq:ode, but the absolute rates depend on target chemistry, cassette design, and extraction not resolved here (§7).

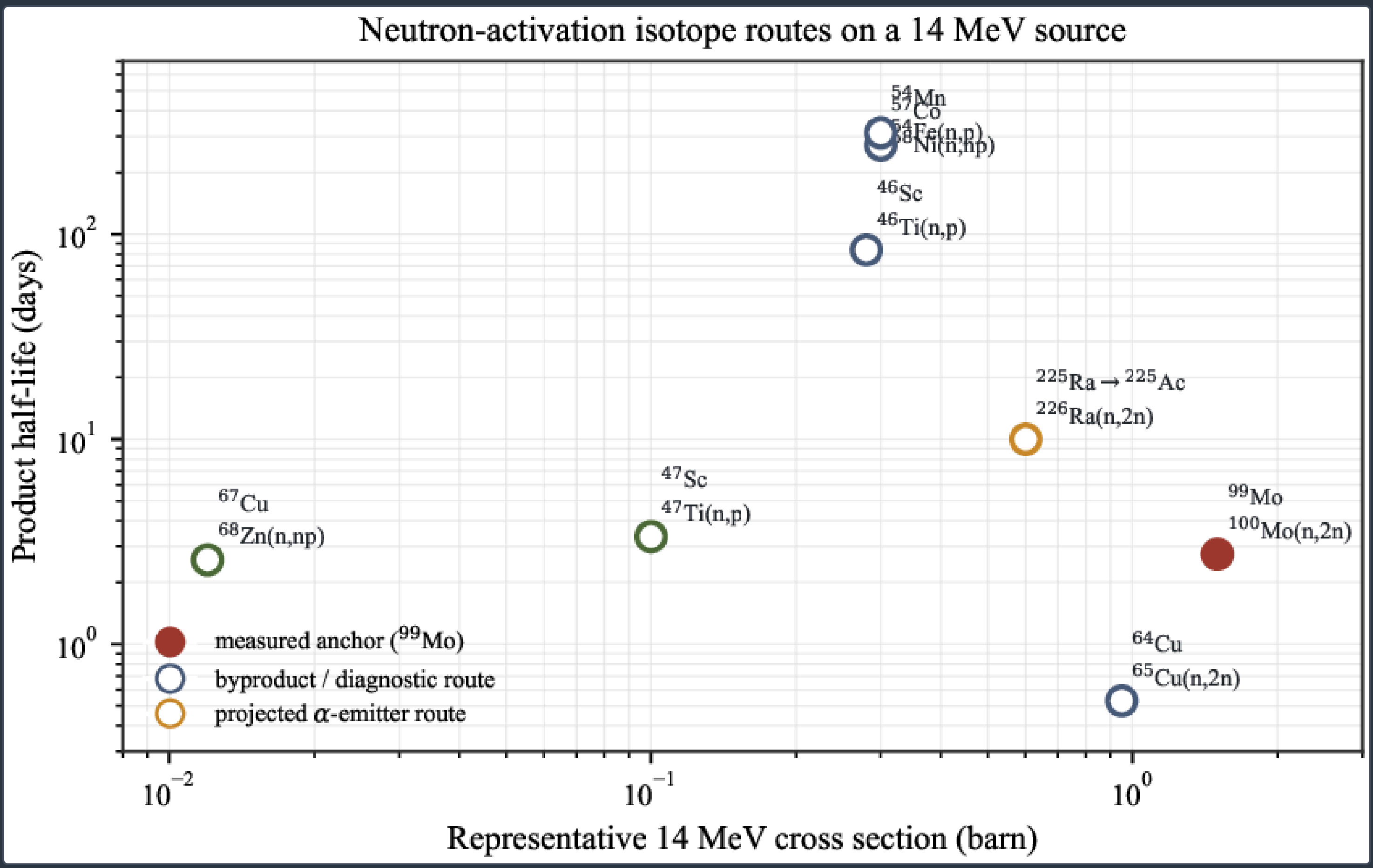

Neutron-activation isotope routes on the 14 MeV source: representative 14 MeV cross-section versus product half-life. Filled marker: the measured ^{99}Mo anchor. Open markers: byproduct and projected α-emitter routes. Cross-section magnitudes are representative ENDF/EAF-class values; only ^{99}Mo is a frozen production anchor.

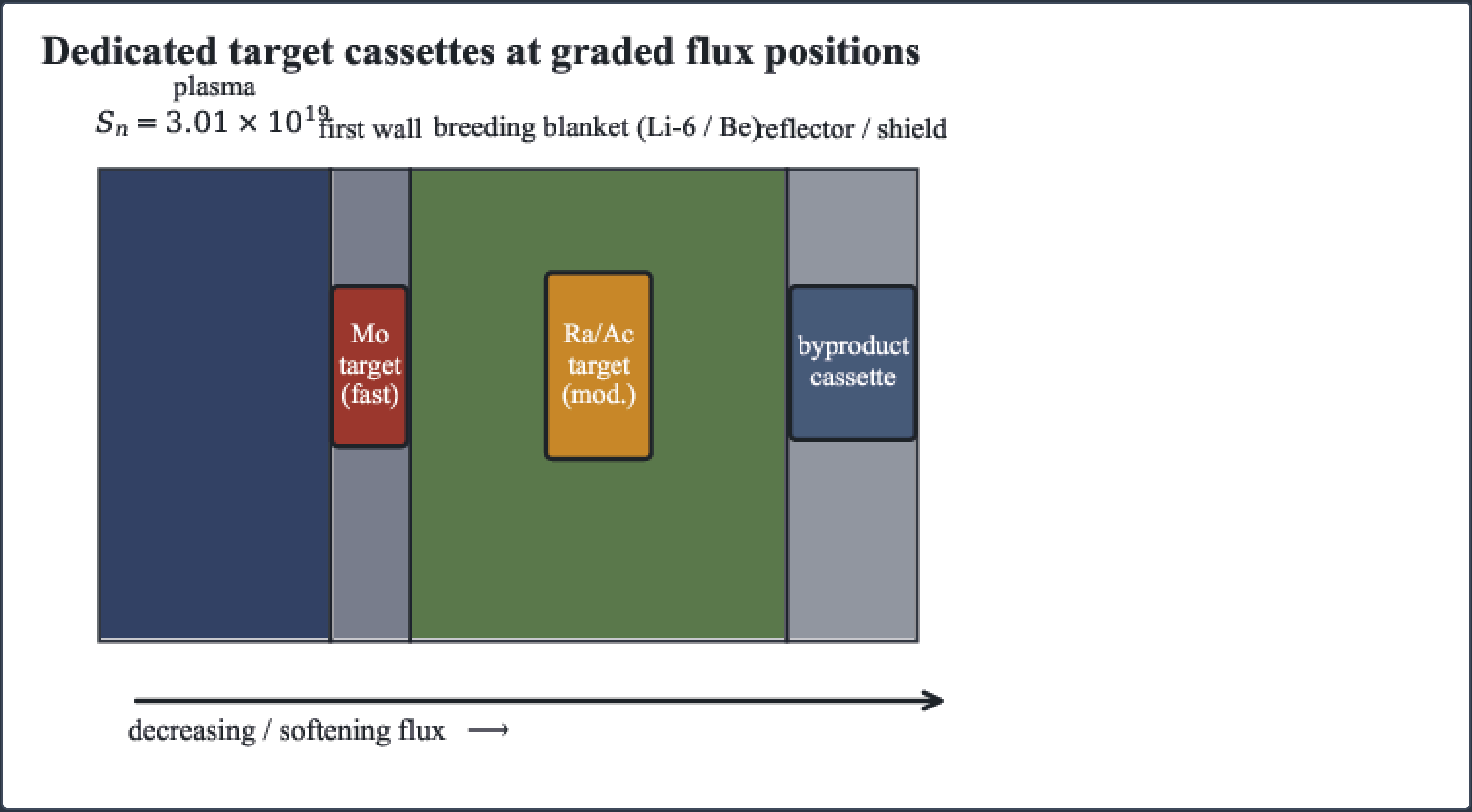

Target cassettes at graded flux positions in the neutron field: a ^{100}Mo cassette in the hard first-wall flux, a moderated Ra/Ac cassette in the blanket, and a byproduct cassette in the reflector, with the flux softening outward. *(Schematic.)*

THE STRATEGIC-OUTPUT LEDGER

Figure 9 assembles the strategic outputs per unit full-power year, booked as capability. The tritium balance is anchored by a fixed burn of $4.77\,\mathrm{kg\text{-}T\,fpy^{-1}}$; at the self-sufficient design blanket (net breeding ratio 1.19) the net tritium is $\approx 0.9\,\mathrm{kg\,fpy^{-1}}$, rising to $\approx 3.8\,\mathrm{kg\,fpy^{-1}}$ at the advanced/isotope-foundry blanket lever (ratio 1.80) [1,7]. The helium-3 co-product is $\approx 0.9\,\mathrm{kg\,yr^{-1}}$ per unit at equilibrium [1,7]. On top of this material ledger sit the $\sim 2\,\mathrm{kCi}$ ^{99}Mo capability per $100\,\mathrm{g}$ target and the $21.6\,\mathrm{L}$, $\geq 10\,\mathrm{dpa\,fpy^{-1}}$ test volume. Fast-ion loss is negligible over this campaign (α confinement 99.98%) and the surrounding alloys return near-neutral in activation [2], so the co-production does not degrade the plasma or the waste posture; the activated target cassettes route through the same low-activation waste-class analysis as the rest of the device, with no isotope beyond a century's half-life [9].

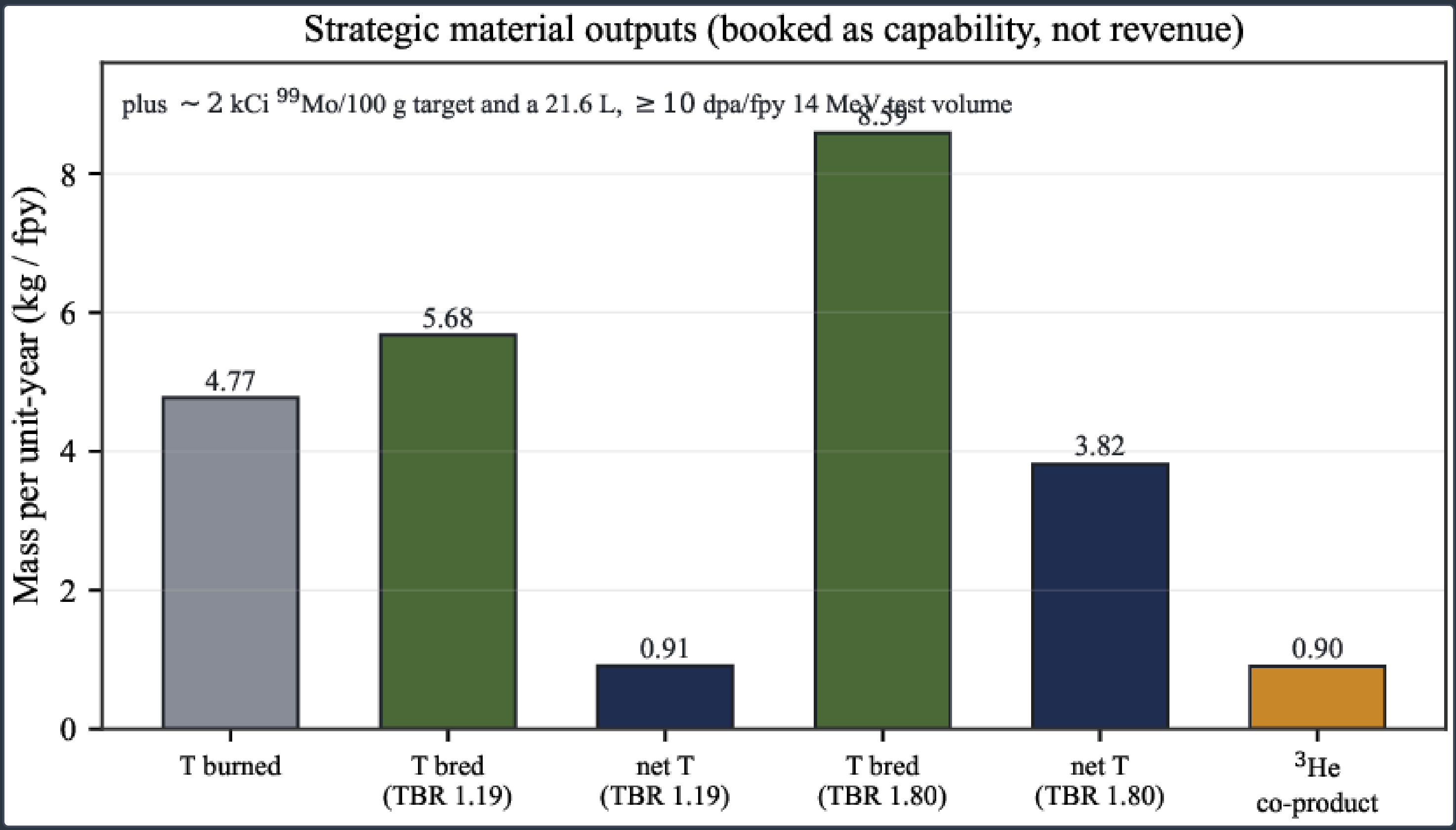

Strategic material outputs per unit-year, booked as capability. Tritium burned ($4.77\,\mathrm{kg\,fpy^{-1}}$), bred and net at two blanket points (ratios 1.19 and 1.80), and the ^{3}He co-product ($0.9\,\mathrm{kg\,yr^{-1}}$), plus the ^{99}Mo and materials-test capability noted in the annotation. No economic quantity is computed.

§ 6

Discussion

Against the medical-isotope literature. The $^{100}\mathrm{Mo}(n,2n)^{99}\mathrm{Mo}$ route was proposed by Nagai and Hatsukawa as a fission-free path to $^{99}\mathrm{Mo}$, and their scoping estimate — $\sim 79\,\mathrm{GBq\,g^{-1}}$ specific activity for a 198-hour irradiation of enriched $^{100}\mathrm{Mo}$ at $\sim 10^{13}\,\mathrm{n\,cm^{-2}\,s^{-1}}$ near $14\,\mathrm{MeV}$ [14] — is the natural benchmark. Our frozen first-wall flux is $\sim 70\times$ higher, and eq:sat then predicts a proportionally higher production rate; the frozen $2.04\,\mathrm{kCi}$ per $100\,\mathrm{g}$ natural target (equivalently $\sim 0.75\,\mathrm{GBq\,g^{-1}}$ on the natural target, or an order of magnitude higher on an enriched target) is fully consistent with the $\sigma \approx 1.5\,\mathrm{b}$ benchmark once the abundance and flux are scaled. The point is not that fusion beats an accelerator at every metric — the specific-activity limitation of the $(n,2n)$ route is intrinsic and shared — but that a power-class breeder delivers the required flux *as a byproduct of its primary mission*, and that a single unit's capability is at the scale of a regional supply. Because the target is non-fissile, the plant sits under a byproduct-material regulatory posture rather than a reactor posture, which is developed in the companion licensing work [6].

Against the materials-source literature. The fusion-materials community has for two decades identified the absence of a high-flux $14\,\mathrm{MeV}$ source as a critical path to a demonstration reactor, and has pursued IFMIF and IFMIF-DONES precisely to fill it [18,19,20]. Those sources deliver the correct spectrum over a high-flux volume of order $0.5\,\mathrm{L}$. Our $21.6\,\mathrm{L}$ at $\geq 10\,\mathrm{dpa\,fpy^{-1}}$ is larger by two-plus orders of magnitude (Fig. 4) because a volumetric plasma source irradiates its entire first wall and near-blanket, not a millimetric beam footprint. The comparison is a like-for-like capability ratio against published facility specifications, not a claim of measured throughput. The value is that structural-alloy qualification — the RAFM steels, the low-activation refractory high-entropy alloys, and the REBCO conductor under fast fluence studied elsewhere in the series [4,5,8] — can be advanced in the same spectrum the components will see in service.

Coupling and co-benefits. The two missions are not independent add-ons; they are consequences of the same source and are bounded by the same constraint eq:opt. The materials-test flux and the isotope-target flux both scale with S_n, and both are capped by centrepost life. This is why we present the source-damage trade (Fig. 6) as a first-class result: it is the honest statement of how hard the co-production can be pushed before the consumable centrepost, not the plasma, becomes the limit.

§ 7

Limitations

One gate is stated plainly. The ^{99}Mo yield is a frozen, computed anchor and is reproduced two ways (§5.1); but the α-emitter and general byproduct yields (§5.3) are *capability projections*, not operating yields. Their governing equation eq:ode is exact, yet the achievable activity of, e.g., ^{225}Ac depends on the ^{226}Ra target form, the moderated-cassette flux and spectrum, radiolysis and self-heating in the target, and a separation chemistry that is not modelled here. The materials-facility multipliers likewise compare a modelled full-rate capability and a modelled $\geq 10\,\mathrm{dpa\,fpy}^{-1}$ volume to published facility specifications, not to measured specimen throughput, and they inherit the nuclear-data uncertainty of the damage cross-sections [8]. These are scoping results from a frozen source, to be confirmed by dedicated target-station and irradiation-campaign design.

§ 8

Conclusion

A compact ST breeder is a bright $14\,\mathrm{MeV}$ neutron source before it is anything else, and that source is a co-production platform. From a single frozen operating point ($P_{\mathrm{fus}} = 85.04\,\mathrm{MW}$, $S_n = 3.01 \times 10^{19}\,\mathrm{n\,s^{-1}}$, $\phi_{\mathrm{fw}} = 7.0 \times 10^{14}\,\mathrm{n\,cm^{-2}\,s^{-1}}$) the device delivers a fission-free ^{100}Mo$(n, 2n)^{99}$Mo route at $\approx 1{,}981\,\mathrm{Ci}$ per $100\,\mathrm{g}$ after 14 days, a genuine fusion-spectrum materials-qualification volume of $21.6\,\mathrm{L}$ at $\geq 10\,\mathrm{dpa\,fpy^{-1}}$ ($315\times$ IFMIF, $630\times$ DONES, and $\approx 59\times$ a reference facility in full-rate capability), and a family of scoped α-emitter and byproduct routes — all bounded by a strict $1{:}1$ source-strength/centrepost-life trade. These are strategic-material co-products of the neutron economy, booked as capability and computed on the NVIDIA GPU HPC campaign, with every headline value a frozen anchor in the de-risking register.

AcknowledgmentstocsectionAcknowledgments

Part of the Kronos Fusion Energy 2026 design series. The authors thank the Kronos physics de-risking programme for the frozen result set underlying every quantitative claim, and G L Kulcinski (co-founder) for the helium-3 and neutron-source framing.

Reproducibility. Every headline quantity is a frozen anchor in the Kronos Physics De-Risking Register [1] (doi:10.5281/zenodo.22133057): the source strength and first-wall flux (gate BR-L1-A5), the wall load and displacement rate (gates BR-L1-A9/A13), the ^{99}Mo$(n, 2n)$ co-production yield (materials & alloys breakthrough gate), the materials-qualification multipliers (closure criterion H-C3), and the helium-3/tritium ledger (gates BR-OUT-2/BR-L1-A6). Each is regenerable from the deposited OpenMC/FISPACT-II runbook and the figure-generation script deposited with this paper; this paper is archived at doi:10.5281/zenodo.22645762; official version: https://www.kronos-fusionenergy.com/publications/isotopes-and-14-mev-applications.html. No result depends on unpublished or proprietary data, and no economic quantity is part of the record.

Data availabilitytocsectionData availability The activation build-up, flux-scaling, capability, spectrum, route-map, and ledger data used for figures 1–9 are generated by the deposited script and trace to the register [1] by the serial identifiers cited inline. This paper is archived at doi:10.5281/zenodo.22645762; the register is deposited at doi:10.5281/zenodo.22133057. Any economic analysis is reported separately and is not part of the public deposit.

Competing intereststocsectionCompeting interests Provisional patent applications relating to aspects of this work have been filed. The authors declare no other competing interests.

tocsectionReferences

APPARATUS

Portfolio, People & Record

The intellectual-property estate, the people who built it, the limitations that gate it, and the sources it rests on.

1	4	40	27
GRANTED PATENT	2026 PROVISIONALS	TEAM MEMBERS	2022 PROVISIONALS

INTELLECTUAL PROPERTY

The patent portfolio

The estate spans a granted high-field magnet patent, pending utility and 2026 provisional filings that map to the two products, a digital-twin control provisional, a registered trademark application, and the original 2022 provisional family. Every patentable disclosure in the five-paper arXiv drop was protected **before** publication: the breeder and burner provisionals were filed 1–2 August, and a publication-gap omnibus filing the evening before the drop swept up the DEC, plasma-control, and REBCO-winding matter of the three otherwise-unprotected papers. Patent numbers and application serials are matters of public record; claim scope is summarised, not reproduced.

GRANTED & PENDING UTILITY

US 12,009,112	High-field tilted graded-REBCO magnet architecture (KRONO-002A) · *app. 17/878,550*	GRANTED
US 17/878,507	Core device / method (KRONO-001A) · *utility*	PENDING

2026 PROVISIONAL FILINGS — MAPPED TO THE PRODUCTS

64/124,209	Hyperion — spherical-tokamak tritium / helium-3 foundry · *breeder · filed Aug 2026*	FILED
64/124,220	Aegis / MetroVolt — synchrotron-cutoff, fuel-selection & plug-winding · *generator · filed Aug 2026*	FILED
64/115,167	KRONOS-CTRL digital-twin plant control · *provisional · filed Jul 2026*	FILED
64/005,440	Integrated spherical-tokamak fusion architecture · *early integrated-architecture filing · filed Mar 2026*	FILED
64/105,530	Negative-triangularity spherical-tokamak architecture · *foundational ST filing · filed Jul 2026*	FILED
64/128,097	Publication-gap omnibus — quasineutral two-species expander DEC · provenance-gated / latency-split plasma control · as-built high-field winding & conductor architecture · *filed 7 Aug 2026, the evening before the arXiv drop*	FILED

TRADEMARK & ORIGIN

FTK-98801894	Kronos Fusion Energy — trademark application	FILED
KR-2022-*	Original provisional family (KR-2022-00001 … 00027) · *27 filings, 2022*	PRIORITY

The narrow, defensible magnet novelty — the specific conductor and the digital-twin winding optimisation, not high-field REBCO as a category — is the commercial core that can earn ahead of any Q > 1 milestone, with markets in fusion magnet supply, MRI/NMR, accelerators, and proton therapy. The claim is scoped honestly: the high field is a *system field* result, not a stand-alone-coil record; the small-bore plug coil is structurally infeasible as a bare winding but resolved by a stress-managed structural shield (feasible-pending-FEA); and the winding-tape experiment returned a *null result*. The value is the method, not a field record.

THE TEAM

Founding partners, board, advisors & auditors

Kronos is built by a bench of advanced-fuel-fusion, high-field-magnet, direct-conversion, and materials specialists, with a board and operations team drawn from defense, national laboratories, and industry. Dates are shown as ranges; where a tenure has ended or is term-ending, the range says so.

FOUNDING PARTNERS — SCIENCE

Dr. Gerald Kulcinski
Co-Founder · Helium-3 & Advanced-Fuel Fusion
UW–Madison · 2023–Present

Dr. Carl Weggel
Chief Scientist / S.M.A.R.T. Design
MIT Alcator Program · 2022–Present

Dr. Robert J. Weggel
Magnetic Field Design
MIT Magnet Lab · 2022–Present

BOARD

Priyanca Ford
Founder & CEO · Executive Board
2022–Present

Bandel Carano
Finance / Strategy
Oak Investment Partners / Stanford · 2025–2026

Patrick Schweiger
Fusion Device Engineering
Oklo / CFS / TerraPower · 2025–Present

SCIENTIFIC ADVISORS

Dr. Steven O. Dean
Fusion Policy & History
DOE / Fusion Power Associates · 2025–Present

Dr. Patrick H. Diamond
Plasma Turbulence & Transport
UC San Diego · 2025–Present

Dr. Jack J. Dongarra
HPC & Numerical Algorithms
Turing Award · 2025–Present

Dr. Nasr M. Ghoniem
Chief Material Scientist
UCLA · 2025–Present

Dr. Siegfried Glenzer
Plasma Physics & Laser Fusion
Stanford / SLAC · 2022–Present

Dr. David A. Hammer
Pulsed-Power Fusion
Cornell · 2025–Present

Dr. Donald A. Spong
Plasma Theory & Confinement
ORNL · 2025–Present

Dr. Curtis Smith
Risk Assessment & Nuclear PRA
MIT / Idaho National Lab · 2025–Present

RADM (Ret.) David Goggins
Naval Engineering & Power-Plant Design
U.S. Navy · 2023–2026

Dr. Konstantin Batygin
Mathematician
Caltech · 2022–2025

Dr. Ruben Fair
Magnet Design / ITER Liaison
PPPL / Jefferson Lab · 2022–2025

Dr. Paul S. Weiss
Materials & Nanotechnology
UCLA · 2022–2025

SCIENTIFIC AUDITORS

Dr. Wilfred A. Cooper
Plasma Equilibrium Theory
EPFL / Swiss Plasma Center · 2025–Present

Dr. Ahmed Hassanein
Plasma–Material Interactions
Purdue / Argonne · 2025–Present

Dr. Patrick E. Hopkins
Extreme Thermal Materials
U. of Virginia · 2025–Present

Dr. Peter Hosemann
Materials Joining & Structural Integrity
UC Berkeley · 2025–Present

Dr. Travis W. Knight
Advanced Nuclear Fuels & Systems
U. of South Carolina · 2025–Present

Dr. Philippe Lebrun
Cryogenics & Magnet Cooling
CERN · 2025–Present

Dr. Nitendra Singh
Nuclear Safety & Fuel Cycle
ITER · 2025–Present

Dr. Guido Van Oost
Magnetic Confinement & Fusion Systems
Ghent University · 2025–Present

Dr. Gary S. Was
Radiation Materials & Structural Integrity
U. of Michigan · 2025–Present

Dr. Ray Sedwick
Direct Energy Conversion
U. of Maryland · 2025

OPERATIONS

Michael Laughlin
Chief Operating Officer
2022–Present

Martin Owens
Chief Strategy Officer
LANL / GE Hitachi · 2022–Present

MG (Ret.) Paul Pardew
Chief Contracting Officer
Army Contracting Command · 2022–Present

David Beck
Fusion Commercialization
U.S. Space Force · 2024–Present

Sushma Bhatia
Environmental & Legislative
Google · 2022–Present

Michael De Frenza
Technology Licensing
2023–Present

MG (Ret.) Robin L. Fontes
Cybersecurity & Defense
Army Cyber Command · 2022–Present

Vijay Gehani
Supply Chain & Components
INOX India · 2024–Present

Jon Michel Greenwood
IT & AI Infrastructure
Live Nation · 2023–Present

Brian C. O'Neill
National Security
CIA / ODNI · 2022–Present

Gen. (Ret.) Gustave F. Perna
DoD Liaison
Operation Warp Speed · 2022–2023

Andrea Romero
Marketing Lead
2022–Present

Legal counsel is retained; those roles are held on the internal roster and are not listed here.

SOURCES

References

1 P I Ford, *Kronos Physics De-Risking Register*, Kronos Fusion Energy 2026 series. doi:10.5281/zenodo.22133057; register paper doi:10.5281/zenodo.22645689.

2 P I Ford and G L Kulcinski, *Hyperion as a strategic-materials platform: gain, tritium breeding, He-3 co-production and 14 MeV neutron output from a compact spherical tokamak*, Kronos Fusion Energy 2026 design series. doi:10.5281/zenodo.22645691

3 P I Ford, *The Kronos strategic-materials platform: an integrated spherical-tokamak breeder and D–^{3}He tandem-mirror burner architecture with a helium-3 flywheel*, Kronos Fusion Energy 2026 design series. doi:10.5281/zenodo.22645764

4 P I Ford and G L Kulcinski, *First-wall and plasma-facing-component lifetime under 14 MeV loading: displacement damage, bubble swelling and erosion in a compact spherical-tokamak breeder*, Kronos Fusion Energy 2026 design series. doi:10.5281/zenodo.22645774

5 P I Ford, *The centrepost life-limiter: fast-fluence, dpa and shielding setting the cartridge-replacement cadence for a compact spherical-tokamak breeder*, Kronos Fusion Energy 2026 design series. doi:10.5281/zenodo.22645708

6 P I Ford, *The sub-100 MW byproduct-material thesis: why a compact spherical-tokamak breeder licenses under NRC 10 CFR Part 30 rather than Part 50*, Kronos Fusion Energy 2026 design series. doi:10.5281/zenodo.22645756

7 P I Ford and G L Kulcinski, *The D–^{3}He fuel cycle does not close indigenously: helium-3 supply, the lunar gate on burner-scale fuel, and the breeder's strategic co-product*, Kronos Fusion Energy 2026 design series. doi:10.5281/zenodo.22645734

8 P I Ford, *Nuclear-data uncertainty quantification for tritium breeding: which 14 MeV cross-section channels set the error bar on the breeding ratio*, Kronos Fusion Energy 2026 design series. doi:10.5281/zenodo.22645777

9 P I Ford, *Component activation, waste-class routing and decommissioning of a low-activation compact spherical-tokamak breeder: no isotope beyond a century's half-life*, Kronos Fusion Energy 2026 design series. doi:10.5281/zenodo.22645846

10 OECD Nuclear Energy Agency, *The Supply of Medical Radioisotopes: 2019 Medical Isotope Demand and Capacity Projection for the 2019–2024 Period*, OECD/NEA, Paris (2019).

11 National Academies of Sciences, Engineering, and Medicine, *Molybdenum-99 for Medical Imaging*, The National Academies Press, Washington DC (2016). doi:10.17226/23563

12 M R A Pillai, A Dash and F F Knapp Jr, Sustained availability of ^{99m}Tc: possible paths forward, *J. Nucl. Med.* **54** 313 (2013). doi:10.2967/jnumed.112.110338

13 R Van Noorden, The medical testing crisis, *Nature* **504** 202 (2013). doi:10.1038/504202a

14 Y Nagai and Y Hatsukawa, Production of ^{99}Mo for nuclear medicine by $^{100}\text{Mo}(n,2n)^{99}\text{Mo}$, *J. Phys. Soc. Jpn.* **78** 033201 (2009). doi:10.1143/JPSJ.78.033201

15 T J Ruth, Accelerating production of medical isotopes, *Nature* **457** 536 (2009). doi:10.1038/457536a

16 A Morgenstern, C Apostolidis, C Kratochwil, M Sathekge, L Krolicki and F Bruchertseifer, An overview of targeted alpha therapy with ^{225}actinium and ^{213}bismuth, *Curr. Radiopharm.* **11** 200 (2018). doi:10.2174/1874471011666180502104524

17 C Kratochwil, F Bruchertseifer, F L Giesel *et al*, ^{225}Ac-PSMA-617 for PSMA-targeted α-radiation therapy of metastatic castration-resistant prostate cancer, *J. Nucl. Med.* **57** 1941 (2016). doi:10.2967/jnumed.116.178673

18 A Moeslang, V Heinzel, H Matsui and M Sugimoto, The IFMIF test facility design, *Fusion Eng. Des.* **81** 863 (2006). doi:10.1016/j.fusengdes.2005.09.055

19 A Ibarra *et al*, The IFMIF-DONES project: preliminary engineering design, *Nucl. Fusion* **58** 105002 (2018). doi:10.1088/1741-4326/aad91f

20 J Knaster, A Moeslang and T Muroga, Materials research for fusion, *Nat. Phys.* **12** 424 (2016).

21 S J Zinkle and L L Snead, Designing radiation resistance in materials for fusion energy, *Annu. Rev. Mater. Res.* **44** 241 (2014). doi:10.1146/annurev-matsci-070813-113627

22 S J Zinkle and G S Was, Materials challenges in nuclear energy, *Acta Mater.* **61** 735 (2013). doi:10.1016/j.actamat.2012.11.004

COLOPHON

How this document was made

The Kronos Fleet — Combined Editorial, 2026 is set in **Fraunces** (display), **Gelasio** (text), and **IBM Plex Mono** (data & equations), carried forward from the Kronos editorial design system.

The figures are rendered at 300 dpi from the deposited generator scripts; the document is composed as a single self-contained file with embedded fonts and imagery, paginated to US Letter, and rendered to PDF through a headless Chromium engine in matched light and dark editions.

Every headline quantity carries an evidence class; withdrawn and restated values are marked as such. Nothing herein is frozen beyond the founder-approved Tier-A set.

Explore it live — turn the interactive 3-D model, run the deposited solvers in the physics validator, and watch the companion film series.

◆

LEGAL NOTICE

Notice, status, and distribution

Conceptual design & simulation study. This document reports a conceptual design and simulation study. It is not a construction commitment, a safety-analysis report, a regulatory filing, or an offer of securities. Forward-looking statements — schedules, costs, market sizes, and performance — are estimates subject to the limitations set out in the Simulations part and may change.

Numbers and their classes. Quantities are reported with evidence classes and case labels; modelled, assumed, and requirement-class values are identified as such and are not to be quoted without their labels.

Public edition. This edition carries the physics and design only; all financial, funding, and defense-commercial content has been removed for public distribution. The scientific text corresponds to the arXiv and journal submissions.

THE 2026 KRONOS SERIES

One programme, many papers

This editorial is one paper in the Kronos 2026 series — a real fusion company's complete, reproducible physics record for a spherical-tokamak breeder and its low-neutron D–^{3}He tandem-mirror burners. Every headline number is a frozen anchor in the Physics De-Risking Register.

Explore the whole programme: the De-Risking Register, the interactive 3-D model, and the physics validator.

KRONOS FUSION ENERGY

The Medical-Isotope Mission of a Compact Spherical-Tokamak Breeder: Mo-99, Targeted-Alpha Emitters, and Byproduct Isotope Co-Production on a 14 MeV Neutron Source

A real fusion company building real machines. Explore the science, live.

Zenodo · doi:10.5281/zenodo.22645762

Read on kronosfusionenergy.com

The Physics De-Risking Register